The Journal of the Acoustical Society of America

MAY 31 2005

Sound transmission across duct constrictions with and without tapered sections

C. K. Lau; S. K. Tang

J. Acoust. Soc. Am. 117, 3679–3685 (2005)
https://doi.org/10.1121/1.1921549

Sound transmission across duct constrictions with and without tapered sections

C. K. Lau and S. K. Tang[a)]
Department of Building Services Engineering, The Hong Kong Polytechnic University, Hong Kong, China

(Received 29 March 2004; revised 29 March 2005; accepted 5 April 2005)

The sound power transmission loss across duct constrictions with linearly tapered sections is studied with the finite element method. Results show that the acoustic energy distributions of transmitted waves at high frequency depend critically on the exit configuration of the constriction. The corresponding strengths of these waves are very much affected by the entrance setup of the constriction. The difference between inlet and outlet impedance of a constriction leads to weaker resonant sound transmission. © *2005 Acoustical Society of America.* [DOI: 10.1121/1.1921549]

PACS numbers: 43.50.Gf, 43.20.Mv [DKW] Pages: 3679–3685

I. INTRODUCTION

Ventilation and air conditioning systems are major sources of noise in modern high-rise commercial buildings. Their noises propagate into the interior of buildings through the ventilation ductwork. However owing to practical reasons, these ductwork systems usually involve many ducted elements, such as constriction, expansion,[1] bending,[2] and tee-junction.[3] The prediction of sound transmission characteristics across these ducted elements is very important and thus, the topic has attracted the attention of many researchers in the past few decades. For instance, Miles[4,5] and Baumeister *et al.*[6] investigated the plane wave propagation across a variable area duct. Silcox and Lester[7] examined sound wave transmission across a conical constriction with a wall slope of 3.6°. Selamet and Easwaran[8] studied the plane wave propagation across a venturi tube of slow area variation in the presence of a mean flow using the stepwise expansion and contraction duct approximation. Cho and Ingard[9] discussed the propagation of higher modes across a constriction of slow and smooth area variation analytically while Hudde[10] examined similar propagation effects inside divergent and convergent sections again by the stepped duct approximation.

A recent study by the authors[11] revealed that the propagation characteristics of the acoustic modes across smooth convergent and divergent sections in an infinitely long duct are very different. However, the corresponding information for sound propagation across duct constrictions and the associated acoustic mode interactions have, to the knowledge of the authors, not been discussed in detail in existing literature unless drastic simplifications of the nonuniform section configurations are made (for instance, Refs. 9 and 10).

Tapering of the inlet and outlet of a constriction is recommended by building services engineers in order to reduce the fluid pressure loss along the ductwork and the level of regeneration noise. This also results in smoother acoustic impedance change than the abrupt constriction and thus diminishes the sound power transmission loss (TL). Since these effects are contradictory, the balance between them must be carefully optimized. However, it is currently uncertain on how the constriction geometry will affect the sound power transmission, especially when nonplanar waves exist in the duct. In addition, constrictions are found inside conventional dissipative silencers with porous materials. It is then essential to understand the sound wave propagation inside rigid wall constrictions before the corresponding effects of the porous materials can be fully understood.

In the present study, sound transmission across a constriction in an infinite duct is investigated by using the finite element method implemented by the software MATLAB. For simplicity, only linearly tapered convergent and divergent sections are studied. It is hoped that the present study will provide a deeper understanding on the sound transmission across constrictions inside ductwork and useful information for improved ductwork design in the future.

II. COMPUTATIONAL DOMAIN AND BOUNDARY CONDITIONS

Figure 1 shows the schematic diagram of the flow constriction adopted in the present study. The origin of the coordinate system is set at the center of the constriction section. For practical reasons, only two-dimensional linearly tapered convergent and divergent sections are considered. The geometry and acoustic excitation are symmetrical about the longitudinal duct axis and thus no asymmetric duct mode can be excited. The tapering angles of the convergent and divergent sections are denoted by ϕ_c and ϕ_d, respectively. The widths of the main duct and the flow constriction are denoted by d and w, respectively. The lengths of the flow constriction, convergent and divergent linearly tapered sections are denoted by L, $L_c[=(d-w)/2\tan\phi_c]$ and $L_d[=(d-w)/2\tan\phi_d]$, respectively. All the length scales are normalized by the width of the main duct d, and the frequency range investigated is up to $kd=9$, where k is the wave number of the sound involved.

The target here is to solve the following inhomogeneous wave equation with unit plane wave excitation:

$$\nabla^2 p + k^2 p = q, \tag{1}$$

[a)]Author to whom correspondence should be addressed; electronic mail: besktang@polyu.edu.hk

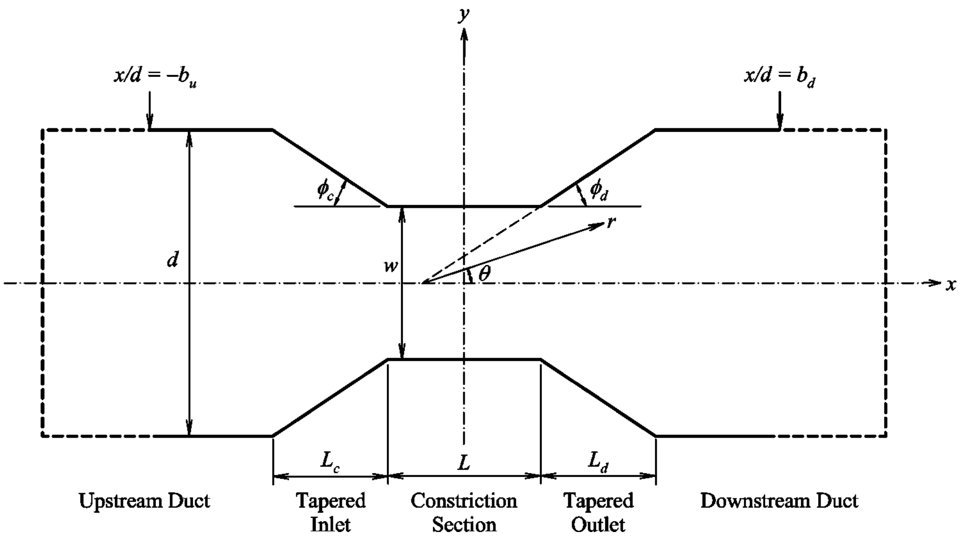

FIG. 1. Schematic diagram of the computational model.

where p and q are the acoustic pressure and sound source strength, respectively, with rigid wall boundaries so that the normal pressure gradients there vanish. For $kd<2\pi$, all the waves in the two straight duct sections are nominally planar. In this case, $q=0$. For a unit-strength acoustic plane wave incident at $x=-b_u$, the boundary conditions at the two ends of the computation domain are

$$\frac{\partial p}{\partial n} \pm ikp = \begin{cases} 2ik, & x=-b_u \\ 0, & x=b_d \end{cases}, \tag{2}$$

where $i=\sqrt{-1}$, n is the outward normal direction of the boundary, b_u and b_d are the computational domain boundary locations (Fig. 1).

When $kd>2\pi$, higher modes are present in the upstream and downstream duct sections. The numerical treatment of Tang and Lau[11] is adopted to damp down the higher modes before they reach the end boundaries (dashed lines in Fig. 1) so as to minimize the numerical reflections there. The boundary conditions of the absorptive side walls are

$$\frac{\partial p}{\partial n} \pm ik\gamma p = 0, \tag{3}$$

where γ is an artificial absorption coefficient which is set at $0.01(x+b_u)^2$ and $0.01(x-b_d)^2$ for upstream and downstream absorptive endings, respectively, as in Tang and Lau.[11] In this case, the unit plane wave excitation is[11]

$$q=2ik\delta(x+b_u), \tag{4}$$

where δ is delta function. Boundary conditions depicted in Eq. (2) apply at the extreme ends of the absorptive endings.

The TL for the plane wave in the present study follows the definition in standard textbook (for instance, Ref. 1). The TL for a higher duct mode is defined as the ratio of the higher mode energy to that of the incident plane wave. The total power transmission loss refers to the ratio of the total energy (plane wave plus higher duct modes) transmitted across the flow constriction to that of the incident plane wave.

All finite element computations are carried out using the partial differential equation (PDE) solver and the mesh generation facilities of the software MATLAB.[12] For each geometry of the constriction, triangular mesh is generated in the computational domain and the PDE (with the determined boundary conditions) is discretized to form a linear system $Ku_h=F$, where the matrices K and F depend on the coefficients of the PDE, and u_h is the unknown vector and contains the values of the approximate solution at the mesh points.

Meshes used in the present study are generated using the Delaunay triangulation algorithm[13] and are refined by the ''regular refinement'' scheme, where all the triangular mesh elements are divided into four triangles.[12] Figure 2 illustrates the computational mesh adopted for the case of $\phi_c=\phi_d$

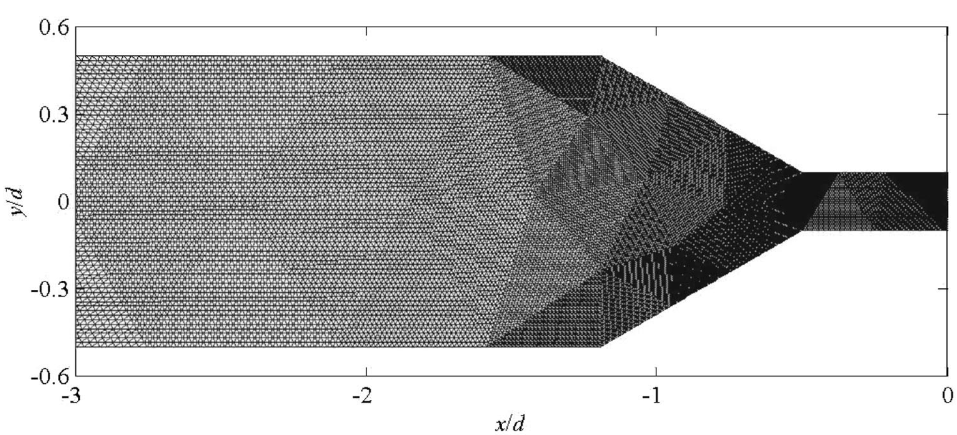

FIG. 2. Computational mesh for $\phi_c=\phi_d=\pi/6$ at $5<kd<9$.

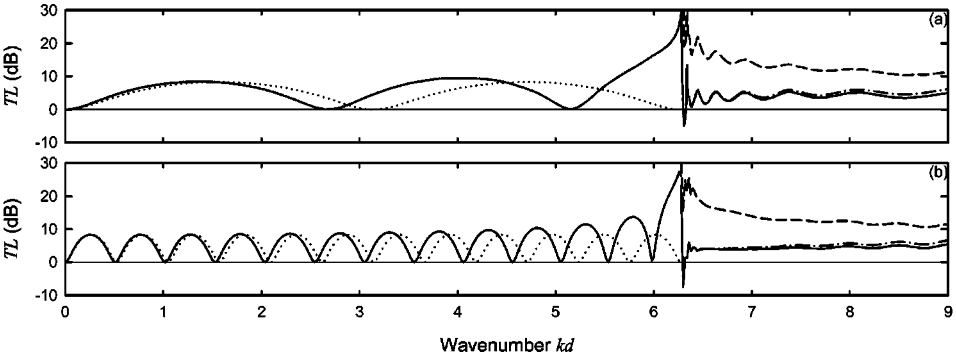

FIG. 3. Sound power transmission loss for constrictions with abrupt contraction and expansion. (a) $L/d=1$, $w/d=0.2$; (b) $L/d=6$, $w/d=0.2$. Plane wave theory $(\cdots)$; total power loss (—); (– – –) plane wave mode power transmission loss for $kd>2\pi$; (–·–) first symmetric higher mode power transmission loss for $kd>2\pi$.

$=\pi/6$ (only those within region $-3\leqslant x/d\leqslant 0$ are presented). The corresponding triangle quality m of each triangle is within 0.7 to ~ 1 which is satisfactory ($m>0.6$ is required[12]). At $kd\sim 9$, the corresponding minimum number of node points $n_{\min}$ per one wavelength of the sound is about 20.

The triangular mesh sizes and details vary with the geometries of the tapered sections and thus are not fixed throughout the investigation. However throughout the computations, m is kept greater than 0.6 and $n_{\min}$ not less than 20. Also, it has been confirmed that further refinement of the meshes will not give noticeable differences in the results.

III. RESULTS AND DISCUSSIONS

The present study investigates the sound wave propagation below the second symmetric cut-on frequency of the duct section ($kd<9$). The TL is estimated from the computed data at $x/d\sim 9$ where all the evanescent waves have been damped out completely.

Owing to the symmetrical excitation and the geometry of the constriction, only symmetrical mode will be excited. For $kd<9$, only the first symmetric mode inside the duct section will be excited while only plane wave propagation is observed inside the constriction section. Inside the tapered section, the corresponding symmetrical mode pattern is[11]

$$[A_\alpha H_\alpha^1(kr)+B_\alpha H_\alpha^2(kr)]\cos(\alpha\theta), \qquad (5)$$

where r and θ are the radial position and the angular position, respectively (Fig. 1), $\alpha=j\pi/\phi$, where j is an integer greater than unity, and A_α and B_α are complex constants. H_α^1 and H_α^2 are the first and second kind Hankel functions of the order α, respectively. θ is bounded between $\pm\phi_c$ or $\pm\phi_d$.

For the convergent inlet, the sound wave begins to propagate in the form of the jth symmetric angular mode if $kd\geqslant 2(j\pi/\phi)\sin\phi$ and can propagate across such section only if

$$kd\geqslant\frac{2j\pi}{\phi}\frac{d}{w}\sin\phi.$$

Sound wave can propagate into the divergent outlet in form of the jth symmetric angular mode if kd satisfies the second requirement of propagation for the convergent inlet.

A. Constrictions with abrupt contraction and expansion

Figures 3(a) and 3(b) illustrate the effects of L/d on the TL across the constriction with abrupt contraction and expansion ($\phi_c=\phi_d=\pi/2$) at $w/d=0.2$. The TLs predicted by the plane wave theory[1] are also given for comparison. The computed TL is comparable to those obtained using the plane wave assumption for all L/d investigated when $kd<2\pi$. However, resonant transmission occurs at lower frequency than the plane wave theory prediction because of the effective length corrections at the two ends of the constriction section due to the radiation impedance there.[1,3]

At $kd\sim 2\pi$ (first symmetric duct mode cut-on frequency), the TL increases; a similar observation was found in the concentric expansion chambers of Selamet and Radvaich.[14] The higher TL near $kd=2\pi$ is due to the strong reflection back into the upstream duct section.

For $kd>2\pi$, the first symmetric higher duct mode is excited. It propagates along the duct sections together with the plane wave. The resulting sound amplification at kd just higher than 2π is due to the strong excitation of the first symmetric higher duct mode. An increase in the length of the constriction results in smaller TL fluctuations for $kd>2\pi$ [Fig. 3(b)]. In all cases with $w/d=0.2$, the higher mode dominates when $kd>2\pi$. The increase in w/d at a fixed L/d reduces the TL across the constriction as expected due to better impedance matching between the duct and the constriction sections. Thus, the associated results are not presented.

Figure 4 shows the sound wave interactions within the proximity of the constriction with abrupt contraction and expansion for $L/d=1$, $w/d=0.2$. At low frequency, the sound waves have circular wave fronts near the inlet and exit of the

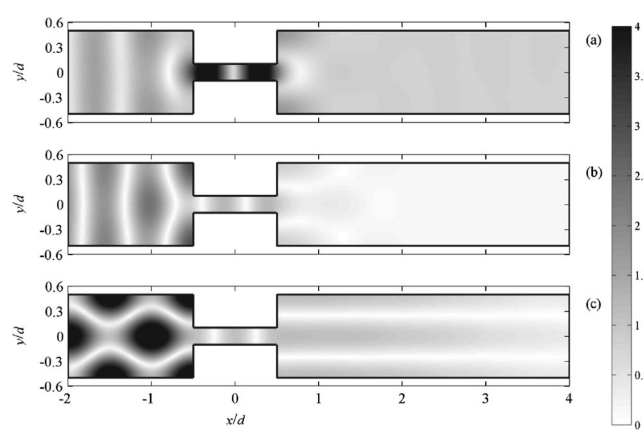

FIG. 4. Sound field patterns around constrictions with abrupt contraction and expansion. (a) $kd=5$; (b) $kd=6$; (c) $kd=6.3$. $w/d=0.2$, $L/d=1$.

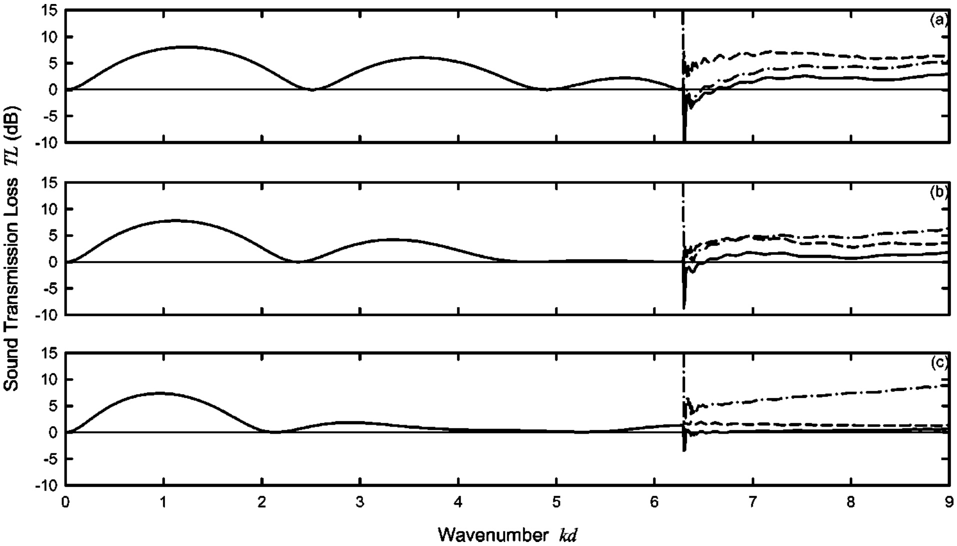

FIG. 5. Sound transmission across constrictions with tapered inlet and outlet. (a) $\phi_c=\phi_d=\pi/3$; (b) $\phi_c=\phi_d=\pi/4$; (c) $\phi_c=\phi_d=\pi/6$. $w/d=0.2$, $L/d=1$. Total power loss (—); plane wave mode power transmission coefficient for $kd>2\pi$ (–––); first symmetric higher mode power transmission coefficient for $kd>2\pi$ (–·–).

constriction [Fig. 4(a)]. These wave fronts then spread out to fill the duct cross section with uniform energy density. At kd just below 2π, the first symmetric higher mode of the duct section is found at the exit plane of the constriction [Fig. 4(b)]. This mode decays rapidly as it propagates into the downstream duct section as expected. Strong acoustic reflection back into the upstream duct occurs resulting in the rapid increase of TL as kd approaches 2π [Fig. 4(b)].

The strong higher mode created by the resonance at $kd>2\pi$ carries the majority of energy into the downstream duct [Fig. 4(c)], resulting in sound amplification (Fig. 3). One should also note that the case of $kd\sim 2\pi$ coincides with one of the resonant transmission cases across the constriction. The sound field patterns at higher kd are similar to that shown in Fig. 4(c), except that more nodal and antinodal planes are observed because of reduced wavelength, and thus are not presented. Away from the resonance frequency, energy is gradually redistributed back to the plane wave mode, causing a reduction in the TL of the plane wave mode shown in Fig. 3 at increased kd.

The phenomena observed in Figs. 3 and 4 are also found in other values of L/d once w/d is fixed (not presented here). Therefore without loss of generality, the foregoing discussions concerning tapered sections are done with $L/d=1$ and $w/d=0.2$, while L_c/d and L_d/d vary with the angles of tapering ϕ_c and ϕ_d.

B. Constrictions with tapered inlet and outlet

With $L/d=1$ and $w/d=0.2$, the effects of ϕ_c ($=\phi_d$ in this section) on the sound transmission across the constriction are shown in Fig. 5. One would expect that a smaller ϕ_c will provide a better acoustic impedance matching between the constriction and the duct sections, resulting in a lower TL than that obtained with abrupt expansion and contraction for $kd<2\pi$. The improvement in such matching increases with frequency and thus the TL dome magnitudes decrease at reduced ϕ_c. At very low frequency where the wavelength of the sound is much longer than the lengths of the tapered sections, the sound wave treats these sections as abrupt contractions and expansions. The TL is thus approximately equal to the plane wave theory prediction. Increasing frequency (reducing the wavelength) allows better development of wave propagation inside the constriction section, resulting in a gradual drop of the TL as kd approaches 2π for a fixed constriction geometry. This situation is enhanced by reducing ϕ_c and thus the magnitudes of the TL domes decrease more rapidly with frequency in such cases. The TL therefore does not rise up when kd approaches 2π as in Fig. 3.

The first symmetric angular mode is excited when $kd=1.65\pi(\sim 5.18)$, $1.8\pi(\sim 5.65)$, and $1.91\pi(\sim 6.00)$ for ϕ_c ($=\phi_d$) equals $\pi/3$, $\pi/4$, and $\pi/6$, respectively. This higher angular mode matches better with the first symmetric higher duct mode and thus the latter is more efficiently excited than in the abrupt expansion case. A higher possibility of sound amplification at $kd\sim 2\pi$ is thus expected. However, the smoother development of the waves inside the tapered sections, especially those within the outlet, provides more uniform acoustic excitation to the duct modes. Figure 5 also illustrates that the contribution of the higher duct mode is reduced while that of the plane wave mode is enhanced as the angle of tapering decreases.

Within the ranges of frequency and angle of tapering in the present study, sound wave cannot propagate through the constriction in the form of the higher angular mode as kd is always below

$$\frac{2j\pi}{\phi}\frac{d}{w}\sin\phi.$$

At $kd\sim 6$, ($>1.65\pi$), the first symmetric angular mode can be observed only at the junction between the duct and the convergent inlet [Fig. 6(a)]. The wave patterns well inside the tapered sections remain very circular. Though the higher duct mode decays as it propagates in the downstream duct section, it penetrates longer into this duct section than in the cases of abrupt expansion [cf. Fig. 4(a)]. A reduction of the angle of tapering lengthens this penetration (not shown here).

At $kd>2\pi$, the first symmetric higher mode propagates in the duct sections. The good matching between the higher modes in the tapered sections and the duct sections is manifested in Fig. 6(b). The strong higher duct mode due to reso-

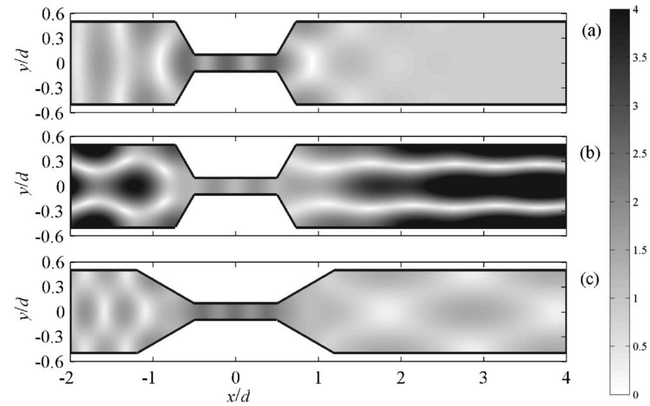

FIG. 6. Sound fields near constrictions with tapered inlet and outlet. (a) $\phi_c=\phi_d=\pi/3$, $kd=6$; (b) $\phi_c=\phi_d=\pi/3$, $kd=6.3$; (c) $\phi_c=\phi_d=\pi/6$, $kd=8$. $w/d=0.2$, $L/d=1$.

nance is also revealed. As the angle of tapering is reduced, the sound pressure magnitude becomes more uniform across the cross section of the downstream duct even at kd far higher than 2π. The diamond shape pattern of the sound field in Fig. 6(c) with its maximum and minimum values on the duct centerline further demonstrates the more dominant plane wave mode at reduced angle of tapering shown in Fig. 5.

C. Constrictions with one end tapered

The constriction with tapered inlet and abrupt expansion ($\phi_d=\pi/2$) produces higher TL (Fig. 7) compared with the one with both tapered inlet and outlet (Fig. 5), but gives lower TL compared with the constriction with abrupt contraction and expansion [Fig. 3(a)]. The maximum TL below the cut-on frequency of the first symmetric higher duct mode is again lowered at smaller ϕ_c. However, it is found that resonant transmission across the constriction becomes less likely here even at a frequency far lower than the first symmetric higher duct mode cut-on frequency as the angle of tapering ϕ_c is reduced. No vanishing TL can be found at $kd>1$ for $\phi_c=\pi/6$ [Fig. 7(b)]. The difference in the inlet and outlet impedance of the constriction creates opposite propagating plane waves of significant different magnitudes such that complete constructive interference cannot take place at the two ends of the constriction region. This is similar to the case of standing wave between two walls of different surface sound absorption.[15]

It is also found from Fig. 7 that the strength of the higher duct mode downstream of the constriction is strong compared to those illustrated in the previous section. The tapered inlet enhances the wave propagation into the constriction and eventually leads to stronger excitation of the higher duct mode at the exit plane of the constriction due to the singularity of the abrupt expansion. Both the strengths of this higher duct mode and the plane wave increase as the angle of tapering decreases as expected, but the former carries a higher percentage of acoustical energy and this percentage increases slightly when the rate of convergence (ϕ_c) is reduced. This is not the case for constrictions with tapered inlet and outlet (Fig. 5). Besides, the smoother convergence leads to the amplification of sound at high frequency [Fig. 7(b)]. The frequency range of such sound amplification is also widened at reduced ϕ_c (not shown here).

For the constrictions with abrupt contraction and tapered outlet ($\phi_c=\pi/2$), the TLs for $kd<2\pi$ are the same as those for the constrictions with tapered inlet and abrupt expansion (Fig. 8). It can also be observed that the TL is always positive here over the frequency range considered in the present study, except at frequencies close to the resonance of the first symmetric higher duct mode. However, the magnitudes and the cycles of the TL oscillations after this resonance are significantly higher than those in Fig. 7. The frequency of the TL oscillation does not appear to depend on ϕ_d. However, the tapered outlet favors energy transfer into the plane wave in the downstream duct section, while the abrupt expansion results in higher energy transfer into the higher duct mode (Figs. 3 and 7).

The relative importance of the higher duct mode at $kd>2\pi$ decreases at reduced ϕ_d. At $\phi_d=\pi/3$ [Fig. 8(a)], both the higher duct mode and the plane wave inside the downstream duct are of comparable magnitudes. As ϕ_d decreases, the more uniform excitation at the exit plane of the tapered outlet appears to favor the propagation of plane wave in the downstream duct [Fig. 8(b)]. This is opposite to what happens in the constrictions with tapered inlet and abrupt expansion, where the singularity at the abrupt expansion outlet favors the excitation of higher duct modes. Under this constriction configuration, the TL is always positive, except when kd is very close to 2π.

The characteristics of the corresponding sound fields for the constrictions with one end tapered are very similar to those presented earlier in this section and thus are not pre-

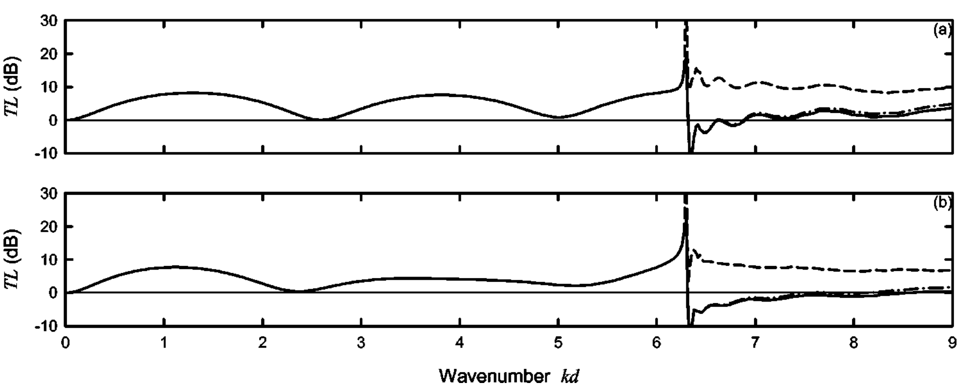

FIG. 7. Sound power transmission loss for constrictions with tapered inlet and abrupt expansion. (a) $\phi_c=\pi/3$, $L_c=0.23$, (b) $\phi_c=\pi/6$, $L_c=0.69$. $\phi_d=\pi/2$, $w/d=0.2$, $L/d=1$. Legends: same as those in Fig. 5.

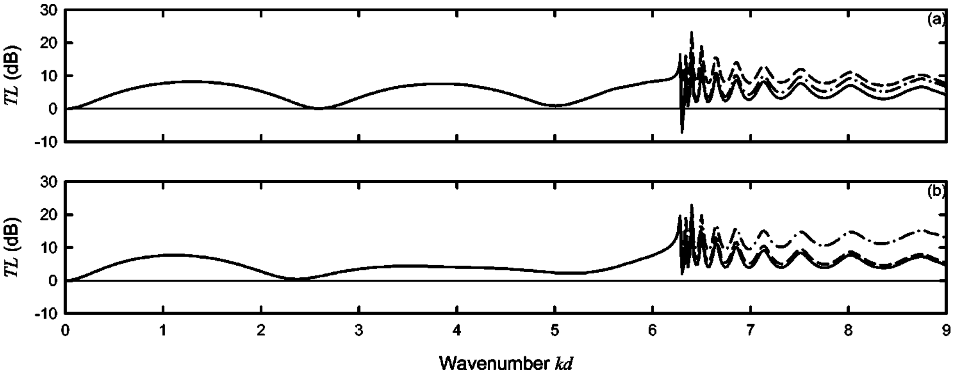

FIG. 8. Sound power transmission loss across constrictions with abrupt contraction and tapered outlet. (a) $\phi_d = \pi/3$, $L_d = 0.23$; (b) $\phi_d = \pi/6$, $L_d = 0.69$. $\phi_c = \pi/2$, $w/d = 0.2$, $L/d = 1$. Legends: same as those in Fig. 5.

sented. The main difference is only the relative magnitudes of the acoustic modes.

IV. PRACTICAL DESIGN CONSIDERATIONS

The tapering of the inlet and outlet of a constriction can reduce the fluid pressure loss and the level of aerodynamic noise generated, but at the same time this reduces the TL. A careful consideration of these effects is essential for practical design.

The pressure loss across the constriction, Δp, in duct can be estimated using

$$\Delta p = [(d/w)^2 C_i + C_o]\rho V^2/2, \tag{6}$$

where ρ is the density of the air, V the mean flow velocity in the main duct, and C_i and C_o the pressure loss coefficients of the inlet and outlet, respectively. According to the pressure-loss coefficients tabulated in ASHRAE,[16] the pressure loss across the convergent inlet is lower than that across the divergent outlet for the same tapering angle. Such difference increases with decreasing w/d. The variation of C_i is very small for $\phi_c < \pi/4$. C_o peaks at around $\phi_d = \pi/4$ and then decreases slowly as ϕ_d increases. Considering the results shown in Figs. 5, 7, and 8, the constrictions with abrupt contraction and tapered outlet appear to be able to give a compromise between the pressure loss and the TL as long as the aeroacoustics is ignored. The abrupt contraction causes smaller pressure loss than the abrupt expansion for $w/d \leqslant 0.5$, but can maintain a more stable and higher TL over the frequency range concerned. Though the abrupt contraction does result in a higher pressure loss than the tapered inlet, the broadband gain in the TL compensates such disadvantage. The constrictions with tapered inlet and abrupt expansion are likely to produce a higher pressure loss without improving the TL. The constrictions with abrupt contraction and expansion give the worst pressure loss without significant improvement in the TL and thus are not desirable.

The corresponding aeroacoustics is complicated. The power of the aerodynamic noise and its frequency depend substantially on the velocity of and the turbulence level in the main flow[17] as well as the geometry of the constriction. This part of the study is very involved and needed to be treated specifically in a separated investigation.

V. CONCLUSIONS

In the present study, the sound power transmission losses through flow constrictions with and without a linearly tapered inlet/outlet in an infinitely long duct are studied with the finite element method. The associated sound energy distributions between various acoustic modes are also discussed.

For the constriction with abrupt contraction and expansion, the computed sound power transmission loss agrees with the plane wave theory prediction at low frequencies. At frequency higher than the first symmetric duct mode cut-on frequency, oscillations of the overall sound power transmission losses are observed. The strength of the plane wave relative to that of the higher duct mode increases at increased frequency, but the latter remains the dominant acoustic mode up to the frequency limit of the present study.

The results in the present study also show that the sound power transmission loss across a flow constriction in an infinitely long duct before the cut-on of the first symmetric higher duct mode is lowered by a smoother constriction transition. Above the cut-on frequency of this higher mode, amplification of sound is likely when the inlet of the constriction is tapered. Such amplification is more significant at reduced tapering angle. Also, the relative importance between the plane wave and the higher duct mode inside the downstream duct depends only on the constriction outlet. For a smoother outlet, the higher mode is more dominant than the plane wave, while the opposite is observed if the constriction consists of an abrupt expansion.

ACKNOWLEDGMENT

This study is supported by a grant from the Research Grant Council, The Hong Kong Special Administration Region, People's Republic of China (Project No. PolyU5030/00E).

[1] L. E. Kinsler and A. R. Frey, *Fundamentals of Acoustics* (Wiley, New York, 1962).
[2] A. Cummings, "Sound transmission in curved duct bends," J. Sound Vib. **35**, 451–477 (1974).
[3] S. K. Tang, "Sound transmission characteristics of Tee-junctions and the associated length corrections," J. Acoust. Soc. Am. **115**, 218–227 (2004).
[4] J. H. Miles, "Acoustic transmission matrix of a variable area duct or nozzle carrying a compressible subsonic flow," J. Acoust. Soc. Am. **69**, 1577–1586 (1981).
[5] J. H. Miles, "Verification of a one-dimensional analysis of sound propa-

gation in a variable area duct without flow,'' J. Acoust. Soc. Am. **72**, 621–624 (1982).
[6] K. J. Baumeister, W. Eversman, R. J. Astley, and J. W. White, ''Acoustics in variable area duct: Finite element and finite difference comparisons to experiment,'' AIAA J. **21**, 193–199 (1983).
[7] R. J. Silcox and H. C. Lester, ''Sound propagation through a variable area duct: Experiment and theory,'' AIAA J. **21**, 1377–1384 (1982).
[8] A. Selamet and V. Easwaran, ''Wave propagation and attenuation in Herschel-Venturi tubes,'' J. Acoust. Soc. Am. **101**, 936–942 (1997).
[9] Y. C. Cho and K. U. Ingard, ''Mode propagation in nonuniform circular ducts with potential flow,'' AIAA J. **21**, 970–977 (1983).
[10] H. Hudde, ''Acoustical higher-order mode scattering matrix of circular nonuniform lossy tubes without flow,'' J. Acoust. Soc. Am. **85**, 2316–2330 (1989).
[11] S. K. Tang and C. K. Lau, ''Sound transmission across a smooth nonuniform section in an infinitely long duct,'' J. Acoust. Soc. Am. **112**, 2602–2611 (2002).
[12] L. Langemyr, A. Nordmark, M. Ringh, A. Ruhe, J. Oppelstrup, and M. Dorobantu, *Partial Differential Equation Toolbox User Guide* (The MathWorks Inc., MA, 1996. The 2004 version is available on-line at http::ww.mathworks.com).
[13] L. P. George, *Automatic mesh generation—Application to Finite Element Methods* (Wiley, New York, 1991).
[14] A. Selamet and P. M. Radavich, ''The effect of length on the acoustic performance of concentric expansion chamber: An analytical, computational and experimental investigation,'' J. Sound Vib. **201**, 407–426 (1997).
[15] H. Kuttruff, *Room Acoustics* (E & FN Spon, New York, 2000).
[16] ASHRAE, *ASHRAE Handbook—Fundamentals* (ASHRAE, Altanta, 2001).
[17] P. O. A. L. Davies, ''Flow-acoustic coupling in ducts,'' J. Sound Vib. **77**, 191–209 (1981).